Electron Beam—Specimen Interactions: Interaction Volume

J. Goldstein et al., *Scanning Electron Microscopy and X-Ray Microanalysis*,
https://doi.org/10.1007/978-1-4939-6676-9_1

1

1.1 What Happens When the Beam Electrons Encounter Specimen Atoms?

By selecting the operating parameters of the SEM electron gun, lenses, and apertures, the microscopist controls the characteristics of the focused beam that reaches the specimen surface: energy (typically selected in the range 0.1–30 keV), diameter (0.5 nm to 1 μm or larger), beam current (1 pA to 1 μA), and convergence angle (semi-cone angle 0.001–0.05 rad). In a conventional high vacuum SEM (typically with the column and specimen chamber pressures reduced below 10^{-3} Pa), the residual atom density is so low that the beam electrons are statistically unlikely to encounter any atoms of the residual gas along the flight path from the electron source to the specimen, a distance of approximately 25 cm.

The initial dimensional scale

With a cold or thermal field emission gun on a high-performance SEM, the incident beam can be focused to 1 nm in diameter, which means that for a target such as gold (atom diameter ~ 288 pm), there are approximately 12 gold atoms in the first atomic layer of the solid within the area of the beam footprint at the surface.

At the specimen surface the atom density changes abruptly to the very high density of the solid. The beam electrons interact with the specimen atoms through a variety of physical processes collectively referred to as "scattering events." The overall effects of these scattering events are to transfer energy to the specimen atoms from the beam electrons, thus setting a limit on their travel within the solid, and to alter the direction of travel of the beam electrons away from the well-defined incident beam trajectory. These beam electron–specimen interactions produce the backscattered electrons (BSE), secondary electrons (SE), and X-rays that convey information about the specimen, such as coarse- and fine-scale topographic features, composition, crystal structure, and local electrical and magnetic fields. At the level needed to interpret SEM images and to perform electron-excited X-ray microanalysis, the complex variety of scattering processes will be broadly classified into "inelastic" and "elastic" scattering.

1.2 Inelastic Scattering (Energy Loss) Limits Beam Electron Travel in the Specimen

"Inelastic" scattering refers to a variety of physical processes that act to progressively reduce the energy of the beam electron by transferring that energy to the specimen atoms through interactions with tightly bound inner-shell atomic electrons and loosely bound valence electrons. These energy loss processes include ejection of weakly bound outer-shell atomic electrons (binding energy of a few eV) to form secondary electrons; ejection of tightly bound inner shell atomic electrons (binding energy of hundreds to thousands of eV) which subsequently results in emission of characteristic X-rays; deceleration of the beam electron in the electrical field of the atoms producing an X-ray continuum over all energies from a few eV up to the beam's landing energy (E_0) (*bremsstrahlung* or "braking radiation"); generation of waves in the free electron gas that permeates conducting metallic solids (plasmons); and heating of the specimen (phonon production). While energy is lost in these inelastic scattering events, the beam electrons only deviate slightly from their current path. The energy loss due to inelastic scattering sets an eventual limit on how far the beam electron can travel in the specimen before it loses all of its energy and is absorbed by the specimen.

To understand the specific limitations on the distance traveled in the specimen imposed by inelastic scattering, a mathematical description is needed of the rate of energy loss (incremental dE, measured in eV) with distance (incremental ds, measured in nm) traveled in the specimen. Although the various inelastic scattering energy loss processes are discrete and independent, Bethe (1930) was able to summarize their collective effects into a "continuous energy loss approximation":

$$\mathrm{d}E/\mathrm{d}s\,(\mathrm{eV/nm}) = -7.85\,(Z\rho/AE)\ln(1.166\,E/J) \qquad \textbf{(1.1a)}$$

where E is the beam energy (keV), Z is the atomic number, ρ is the density (g/cm^3), A is the atomic weight (g/mol), and J is the "mean ionization potential" (keV) given by

$$J\,(\mathrm{keV}) = \left(9.76\,Z + 58.5\,Z^{-0.19}\right)\mathrm{x}\,10^{-3} \qquad \textbf{(1.1b)}$$

The Bethe expression is plotted for several elements (C, Al, Cu, Ag, Au) over the range of "conventional" SEM operating energies, 5–30 keV in Fig. 1.1. This figure reveals that the rate of energy loss dE/ds increases as the electron energy decreases and increases with the atomic number of the target. An electron with a beam energy of 20 keV loses energy at approximately 10 eV/nm in Au, so that if this rate was constant, the total path traveled in the specimen would be approximately 20,000 eV/(10 eV/nm) = 2000 nm = 2 μm. A better estimate of this electron "Bethe range" can be made by explicitly considering the energy dependence of dE/ds through integration of the Bethe expression, Eq. 1.1a, from the incident energy down to a lower cut-off energy (typically ~ 2 keV due to limitations on the range of applicability of the Bethe expression; see further discussion below). Based on this calculation, the Bethe range for the selection of elements is shown in Fig. 1.2. At a particular incident beam energy, the Bethe range decreases as the atomic number of the target increases, while for a particular target, the Bethe range increases as the incident beam energy increases.

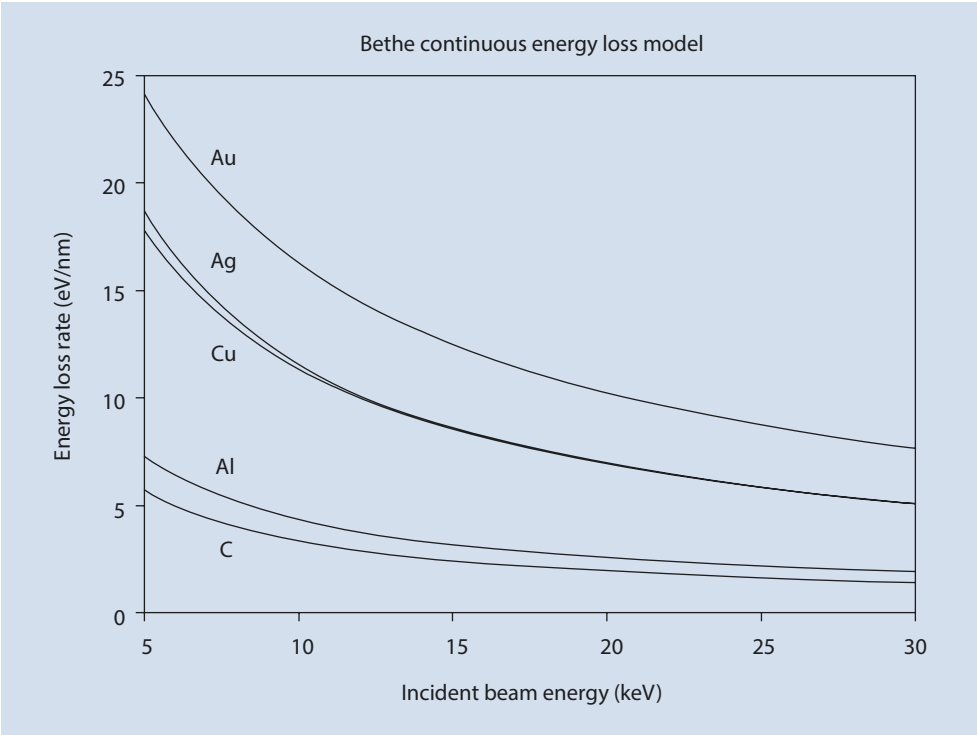

Fig. 1.1 Bethe continuous energy loss model calculations for dE/ds in C, Al, Cu, Ag, and Au as a function of electron energy

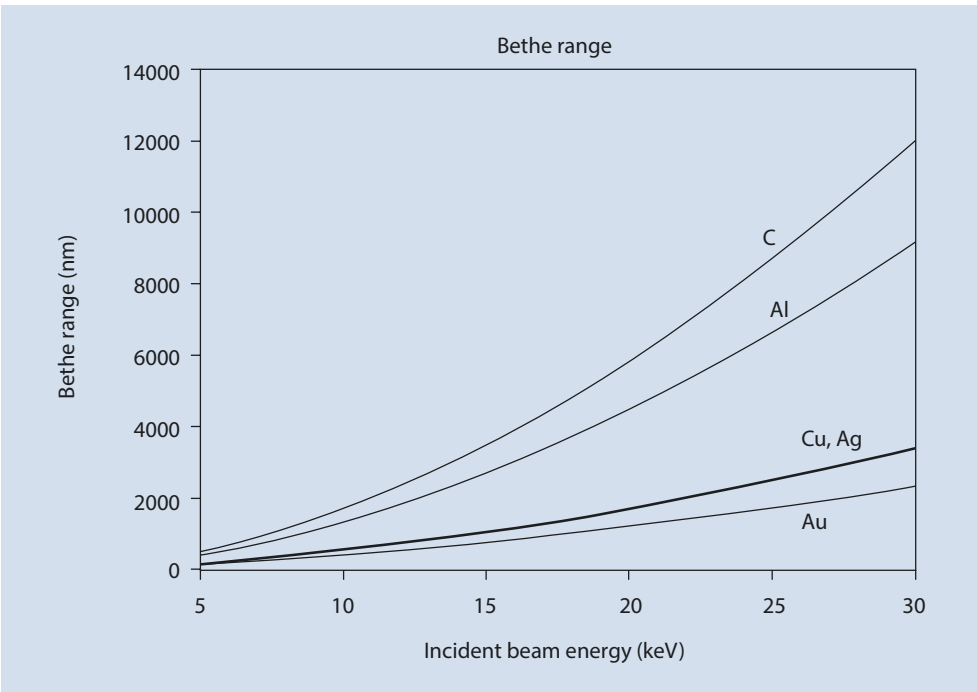

Fig. 1.2 Bethe range calculation from the continuous energy loss model by integrating over the range of energy from E_0 down to a cut-off energy of 2 keV

Note the change of scale

The Bethe range for Au with an incident beam energy of 20 keV is approximately 1200 nm, a linear change in scale of a factor of 1200 over an incident beam diameter of 1 nm. If the beam–specimen interactions were restricted to a cylindrical column with the circular beam entrance footprint as its cross section and the Bethe range as its altitude, the volume of a cylinder 1 nm in diameter and 1200 nm deep would be approximately 940 nm^3, and the number of gold atoms it contained would be approximately 7.5×10^4, which can be compared to the incident beam footprint surface atom count of approximately 12.

1

1.3 Elastic Scattering: Beam Electrons Change Direction of Flight

Simultaneously with inelastic scattering, "elastic scattering" events occur when the beam electron is deflected by the electrical field of an atom (the positive nuclear charge as partially shielded by the negative charge of the atom's orbital electrons), causing the beam electron to deviate from its previous path onto a new trajectory, as illustrated schematically in Fig. 1.3a. The probability of elastic scattering depends strongly on the nuclear charge (atomic number Z) and the energy of the electron, E (keV) and is expressed mathematically as a cross section, Q:

$$Q_{\text{elastic}(>\phi_0)} = 1.62\times10^{-20}\left(Z^2/E^2\right)\cot^2\left(\phi_0/2\right) \left[\text{events} > \phi_0 / \left[\text{electron}\left(\text{atom}/\text{cm}^2\right)\right]\right] \quad (1.2)$$

where ϕ_0 is a threshold elastic scattering angle, for example, 2°. Despite the angular deviation, the beam electron energy is effectively unchanged in energy. While the average elastic scattering event causes an angular change of only a few degrees, deviations up to 180° are possible in a single elastic scattering event. Elastic scattering causes beam electrons to deviate out of the narrow angular range of incident trajectories defined by the convergence of the incident beam as controlled by the electron optics.

1.3.1 How Frequently Does Elastic Scattering Occur?

The elastic scattering cross section, Eq. 1.2, can be used to estimate how far the beam electron must travel on average to experience an elastic scattering event, a distance called the "mean free path," λ:

$$\lambda_{\text{elastic}}\left(\text{cm}\right) = A / \left[N_0 \rho Q_{\text{elastic}(>\phi_0)}\right] \quad (1.3a)$$

$$\lambda_{\text{elastic}}\left(\text{nm}\right) = 10^7 A / \left[N_0 \rho Q_{\text{elastic}(>\phi_0)}\right] \quad (1.3b)$$

where A is the atomic weight (g/mol), N_0 is Avogadro's number (atoms/mol), and ρ is the density (g/cm^3). Figure 1.4 shows a plot of λ_{elastic} for various elements as a function of electron energy, where it can be seen that the mean free path is of the order of nm. Elastic scattering is thus likely to occur hundreds to thousands of times along a Bethe range of several hundred to several thousand nanometers.

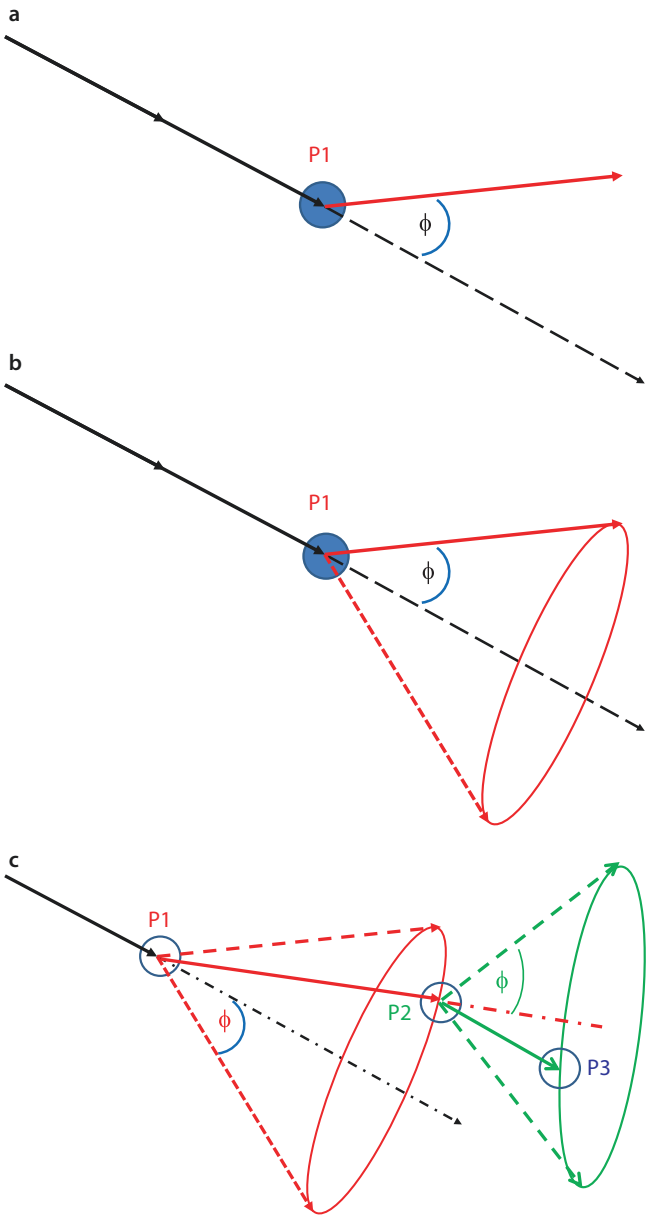

Fig. 1.3 **a** Schematic illustration of elastic scattering. An energetic electron is deflected by the electrical field of an atom at location P1 through an angle ϕ_{elastic}. **b** Schematic illustration of the elastic scattering cone. The energetic electron scatters elastically at point P1 and can land at any location on the circumference of the base of the cone with equal probability. **c** Schematic illustration of a second scattering step, carrying the energetic electron from point P2 to point P3

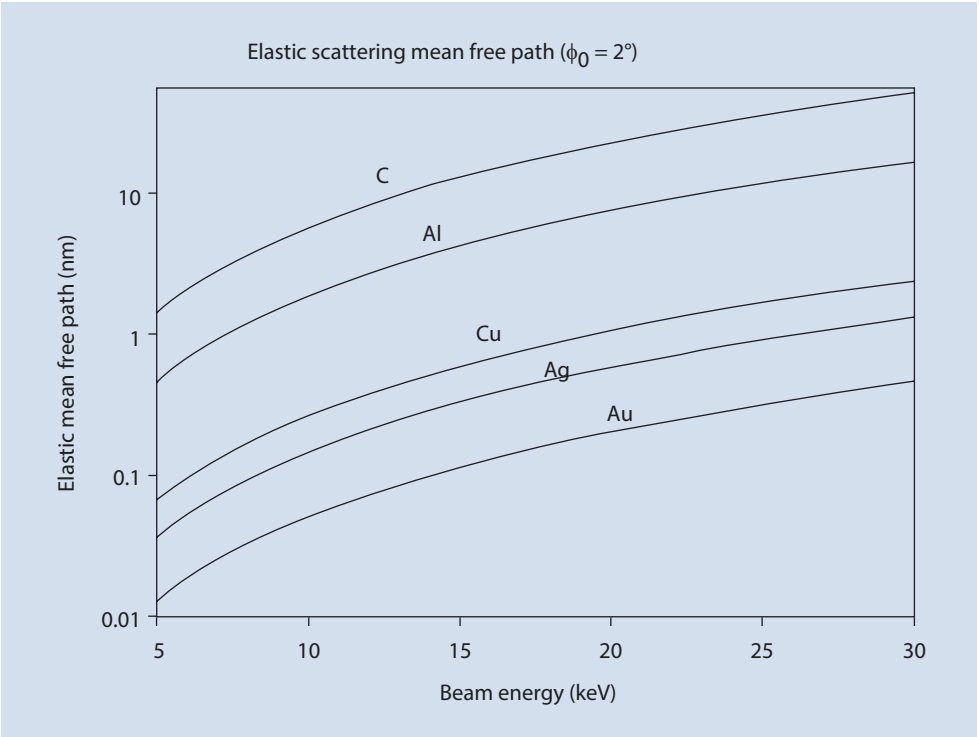

Fig. 1.4 Elastic mean free path as a function of electron kinetic energy for various elements

1.4 Simulating the Effects of Elastic Scattering: Monte Carlo Calculations

Inelastic scattering sets a limit on the total distance traveled by the beam electron. The Bethe range is an estimate of this distance and can be found by integrating the Bethe continuous energy loss expression from the incident beam energy E_0 down to a low energy limit, for example, 2 keV. Estimating the effects of elastic scattering on the beam electrons is much more complicated. Any individual elastic scattering event can result in a scattering angle within a broad range from a threshold of a fraction of a degree up to 180°, with small scattering angles much more likely than very large values and an average value typically in the range 5–10°. Moreover, the electron scattered by the atom through an angle ϕ in Fig. 1.3a at point P1 can actually follow any path along the surface of the three-dimensional scattering cone shown in Fig. 1.3b and can land anywhere in the circumference of the base of the scattering cone (i.e., the azimuthal angle in the base of the cone ranges from 0 to 360° with equal probability), resulting in a three-dimensional path. The length of the trajectory along the surface of the scattering cone depends on the frequency of elastic events with distance traveled and can be estimated from Eq. 1.3a for the elastic scattering mean free path, $\lambda_{elastic}$. The next elastic scattering event P2 causes the electron to deviate in a new direction, as shown in Fig. 1.3c, creating an increasingly complex path. Because of the random component of scattering at each of many steps, this complex behavior cannot be adequately described by an algebraic expression like the Bethe continuous energy loss equation. Instead, a stepwise simulation of the electron's behavior must be constructed that incorporates inelastic and elastic scattering. Several simplifications are introduced to create a practical "Monte Carlo electron trajectory simulation":

1. All of the angular deviation of the beam electron is ascribed to elastic scattering. A mathematical model for elastic scattering is applied that utilizes a random number (hence the name "Monte Carlo" from the supposed randomness of gambling) to select a properly weighted value of the elastic scattering angle out of the possible range (from a threshold value of approximately 1° to a maximum of 180°). A second random number is used to select the azimuthal angle in the base of the scattering cone in Fig. 1.1c.
2. The distance between elastic scattering events, s, which lies on the surface of the scattering cone in Fig. 1.3b, is calculated from the elastic mean free path, Eq. 1.3b.
3. Inelastic scattering is calculated with the Bethe continuous energy loss expression, Eq. 1.1b. The specific energy loss, ΔE, along the path, s, in the surface of the scattering cone, Fig. 1.3b, is calculated with the Bethe continuous energy loss expression: $\Delta E = (dE/ds)^* s$

Given a specific set of these parameters, the Monte Carlo electron trajectory simulation utilizes geometrical expressions to calculate the successive series of locations *P*1, *P*2, *P*3, etc., successively determining the coordinate locations (*x, y, z*) that the energetic electron follows within the solid. At each location *P*, the newly depreciated energy of the electron is known, and after the next elastic scattering angle is calculated, the new velocity vector components v_x, v_y, v_z are determined to transport the electron to the next location. A trajectory ends when either the electron energy falls below a threshold of interest (e.g., 1 keV), or else the path takes it outside the geometric bounds of the specimen, which is determined by comparing the current location (*x, y, z*) with the specimen boundaries. The capability of simulating electron beam interactions in specimens with complex geometrical shapes is one of the major strengths of the Monte Carlo electron trajectory simulation method.

Monte Carlo electron trajectory simulation can provide visual depictions as well as numerical results of the beam–specimen interaction, creating a powerful instructional tool for studying this complex phenomenon. Several powerful Monte Carlo simulations appropriate for SEM and X-ray microanalysis applications are available as free resources:

CASINO [►http://www.gel.usherbrooke.ca/casino/What.html]

Joy Monte Carlo [►http://web.utk.edu/~srcutk/htm/simulati.htm]

NIST DTSA-II [►http://www.cstl.nist.gov/div837/837.02/epq/dtsa2/index.html]

While the static images of Monte Carlo simulations presented below are useful instructional aids, readers are encouraged to perform their own simulations to become familiar with this powerful tool, which in more elaborate implementations is an important aid in understanding critical aspects of SEM imaging.

1.4.1 What Do Individual Monte Carlo Trajectories Look Like?

Perform a Monte Carlo simulation (CASINO simulation) for copper with a beam energy of 20 keV and a tilt of 0° (beam perpendicular to the surface) for a small number of trajectories, for example, 25. Figure 1.5a, b show two simulations of 25 trajectories each. The trajectories are actually determined in three dimensions (*x-y-z*, where *x-y* defines the surface plane and z is perpendicular to the surface) but for plotting are rendered in two dimensions (*x-z*), with the third dimension y projected onto the *x-z* plane. (An example of the true three-dimensional trajectories, simulated with the Joy Monte Carlo, is shown in Fig. 1.6, in which a small number of trajectories (to minimize overlap) have been rendered as an anaglyph stereo representation with the convention left eye = red filter. Inspection of this simulation shows the y motion of the electrons in and out of the *x-z* plane.) The stochastic nature of the interaction imposed by the nature of elastic scattering is readily apparent in the great variation among the individual trajectories seen in Fig. 1.5a, b. It quickly becomes clear that individual beam electrons follow a huge range of paths and simulating a small number of trajectories does not provide an adequate view of the electron beam specimen interaction.

1.4.2 Monte Carlo Simulation To Visualize the Electron Interaction Volume

To capture a reasonable picture representation of the *electron interaction volume*, which is the region of the specimen in which the beam electrons travel and deposit energy, it is necessary to calculate many more trajectories. Figure 1.5c shows the simulation for copper, $E_0 = 20$ keV at 0° tilt extended to 500 trajectories, which reveals the full extent of the electron interaction volume. Beyond a few hundred trajectories, superimposing the three-dimensional trajectories to create a two-dimensional representation reaches diminishing returns due to overlap of the plotted lines. While simulating 500 trajectories provides a reasonable qualitative view of the electron interaction volume, Monte Carlo calculations of numerical properties of the interaction volume and related processes, such as electron backscattering (discussed in the backscattered electron module), are subject to statistically predictable variations because of the use of random numbers to select the elastic scattering parameters. Variance in repeated simulations of the same starting conditions is related to the number of trajectories and can be described with the properties of the Gaussian (normal) distribution. Thus the precision, *p*, of the calculation of a parameter of the interaction is related to the total number of simulated trajectories, *n*, and the fraction, *f*, of those trajectories that produce the effect of interest (e.g., backscattering):

$$p = (fn)^{1/2} / (fn) = (fn)^{-1/2} \tag{1.4}$$

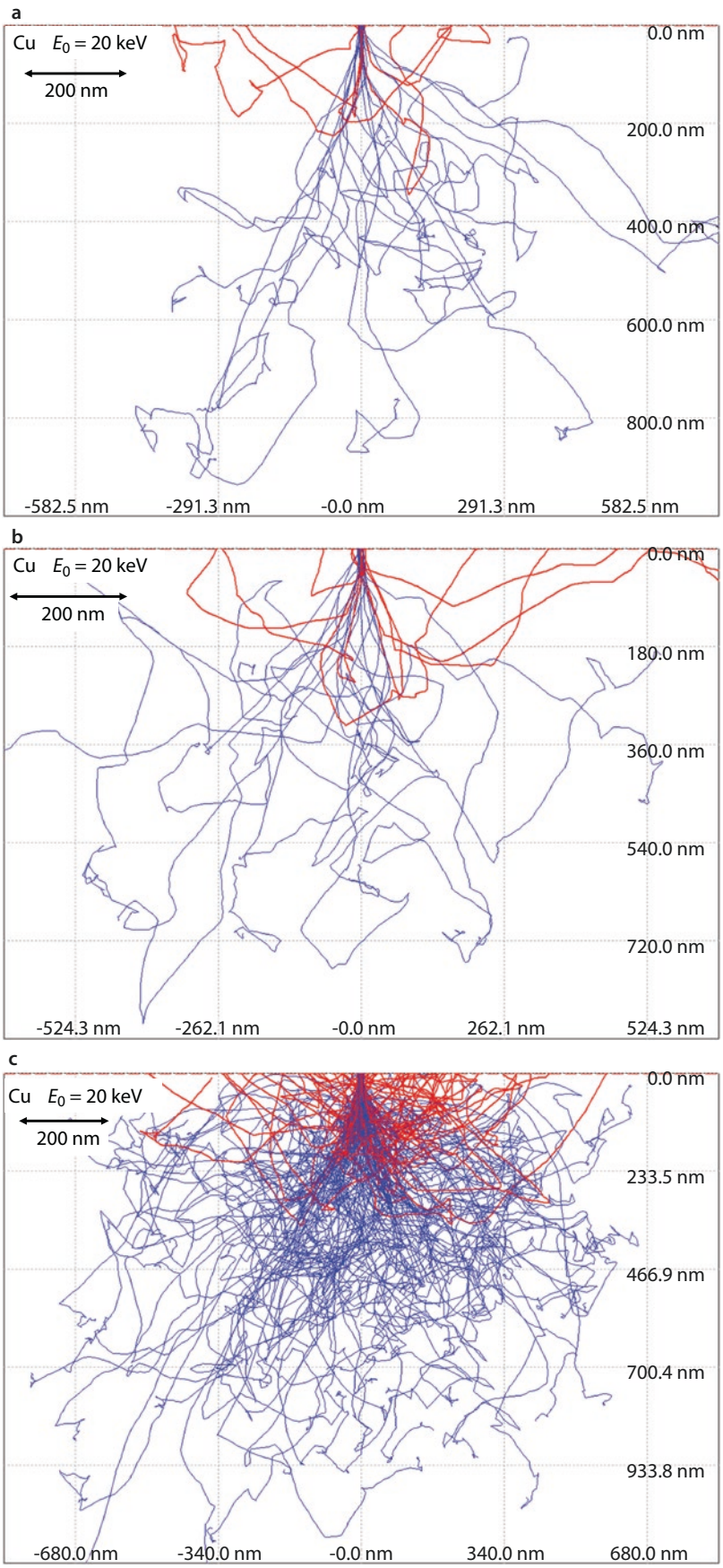

Fig. 1.5 **a** Copper, $E_0 = 20$ keV; 0 tilt; 25 trajectories (CASINO Monte Carlo simultion). **b** Copper, $E_0 = 20$ keV; 0 tilt; another 25 trajectories. **c** Copper, $E_0 = 20$ keV; 0 tilt; 200 trajectories

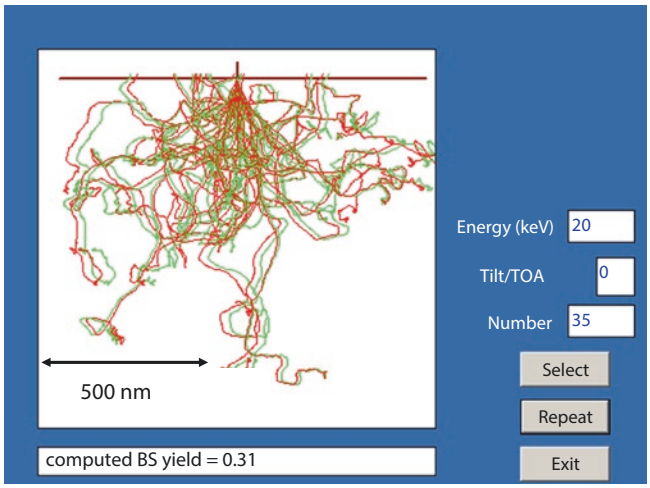

Fig. 1.6 Three-dimensional representation of a Monte Carlo simulation (Cu, 20 keV, 0° tilt) using the anaglyph stereo method (left eye = red filter) (Joy Monte Carlo)

1.4.3 Using the Monte Carlo Electron Trajectory Simulation to Study the Interaction Volume

What Are the Main Features of the Beam Electron Interaction Volume?

In Fig. 1.5c, the beam electron interaction volume is seen to be a very complex structure with dimensions extending over hundreds to thousands of nanometers from the beam impact point, depending on target material and the beam energy. At 0° tilt, the interaction volume is rotationally symmetric around the beam. While the electron trajectories provide a strong visual representation of the interaction volume, more informative numerical information is needed. The Monte Carlo simulation can provide detailed information on many aspects of the electron beam–specimen interaction. The color-encoding of the energy deposited along each trajectory, as implemented in the Joy Monte Carlo shown in Fig. 1.11, creates a view that reveals the general three-dimensional complexity of energy deposition within the interaction volume. The CASINO Monte Carlo provides an even more detailed view of energy deposition, as shown in Fig. 1.7. The energy deposition per unit volume is greatest just under the beam impact location and rapidly falls off as the periphery of the interaction volume is approached. This calculation reveals that a small cylindrical volume under the beam impact point, shown in more detail in Fig. 1.7b, receives half of the total energy deposited by the beam in the specimen (that is, the volume within the 50% contour), with the balance of the energy deposited in a strongly non-linear fashion in the much larger portion of the interaction volume.

How Does the Interaction Volume Change with Composition?

Figure 1.8 shows the interaction volume in various targets, C, Si, Cu, Ag, and Au, at fixed beam energy, $E_0 = 20$ keV, and 0° tilt. As the atomic number of the target increases, the linear dimensions of the interaction volume decrease. The form also changes from pear-shaped with a dense conical region below the beam impact for low atomic number targets to a more hemispherical shape for high atomic number targets.

Note the dramatic change of scale

Approximately 12 gold atoms were encountered within the footprint of a 1-nm diameter at the surface. Without considering the effects of elastic scattering, the Bethe range for Au at an incident beam energy of 20 keV limited the penetration of the beam to approximately 1200 nm and a cylindrical volume of approximately 940 nm^3, containing approximately 5.6×10^4 Au atoms. The effect of elastic scattering is to create a three-dimensional hemispherical interaction volume with a radius of approximately 600 nm and a volume of 4.5×10^8 nm^3, containing 2.7×10^{10} Au atoms, an increase of nine orders-of-magnitude over the number of atoms encountered in the initial beam footprint on the surface.

How Does the Interaction Volume Change with Incident Beam Energy?

Figure 1.9 shows the interaction volume for copper at 0° tilt over a range of incident beam energy from 5 to 30 keV. The shape of the interaction volume is relatively independent of beam energy, but the size increases rapidly as the incident beam energy increases.

How Does the Interaction Volume Change with Specimen Tilt?

Figure 1.10 shows the interaction volume for copper at an incident beam energy of 20 keV and a series of tilt angles. As the tilt angle increases so that the beam approaches the surface at a progressively more shallow angle, the shape of the interaction volume changes significantly. At 0° tilt, the interaction volume is rotationally symmetric around the beam, but as the tilt angle increases the interaction volume becomes asymmetric, with the dense portion of the distribution shifting progressively away from the beam impact point. The maximum penetration of the beam is reduced as the tilt angle increases.

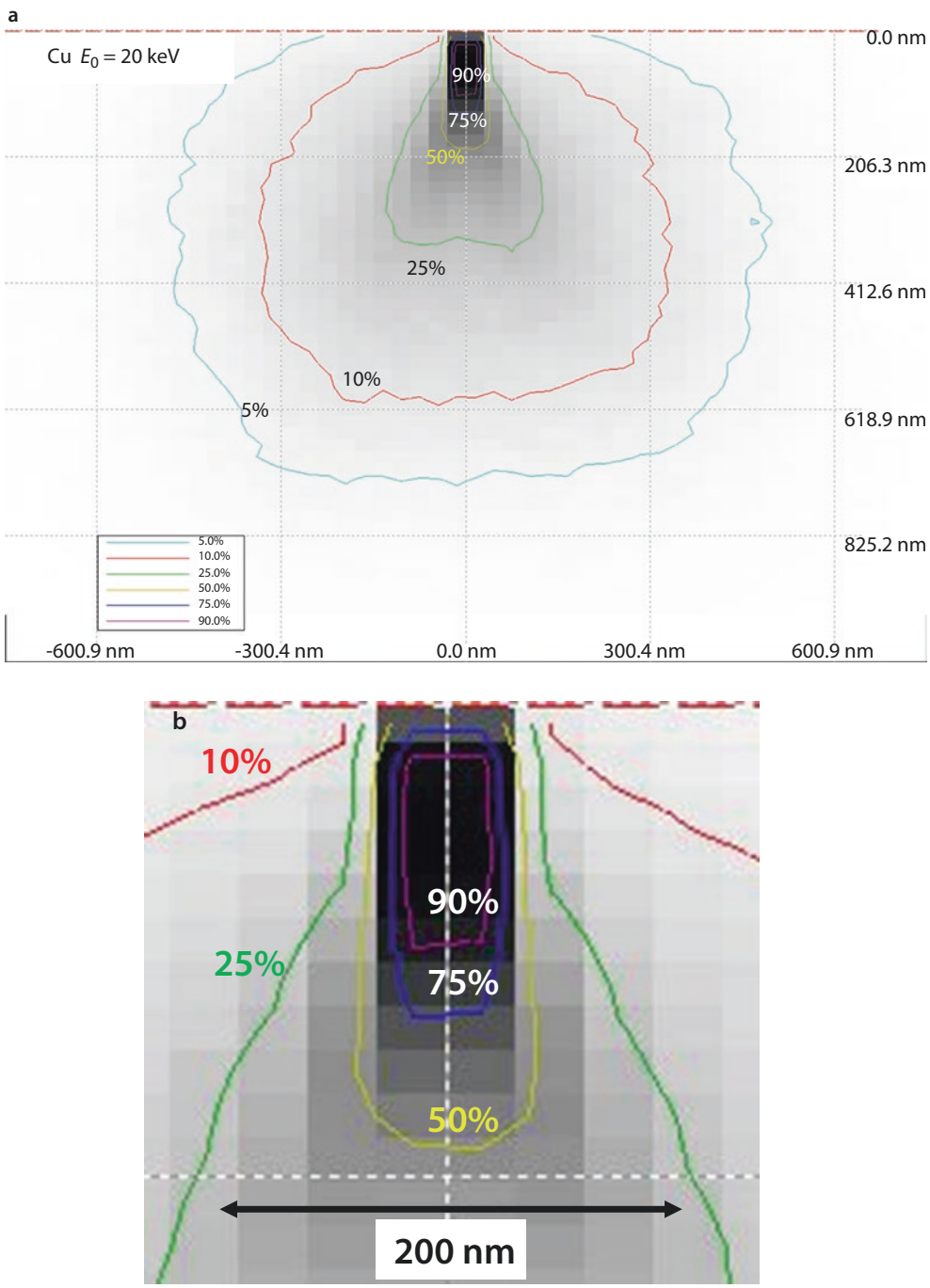

Fig. 1.7 **a** Isocontours of energy loss showing fraction remaining; Cu, 20 keV, 0° tilt; 50,000 trajectories (CASINO Monte Carlo simulation). **b** Expanded view of high density region of 1.7**a**

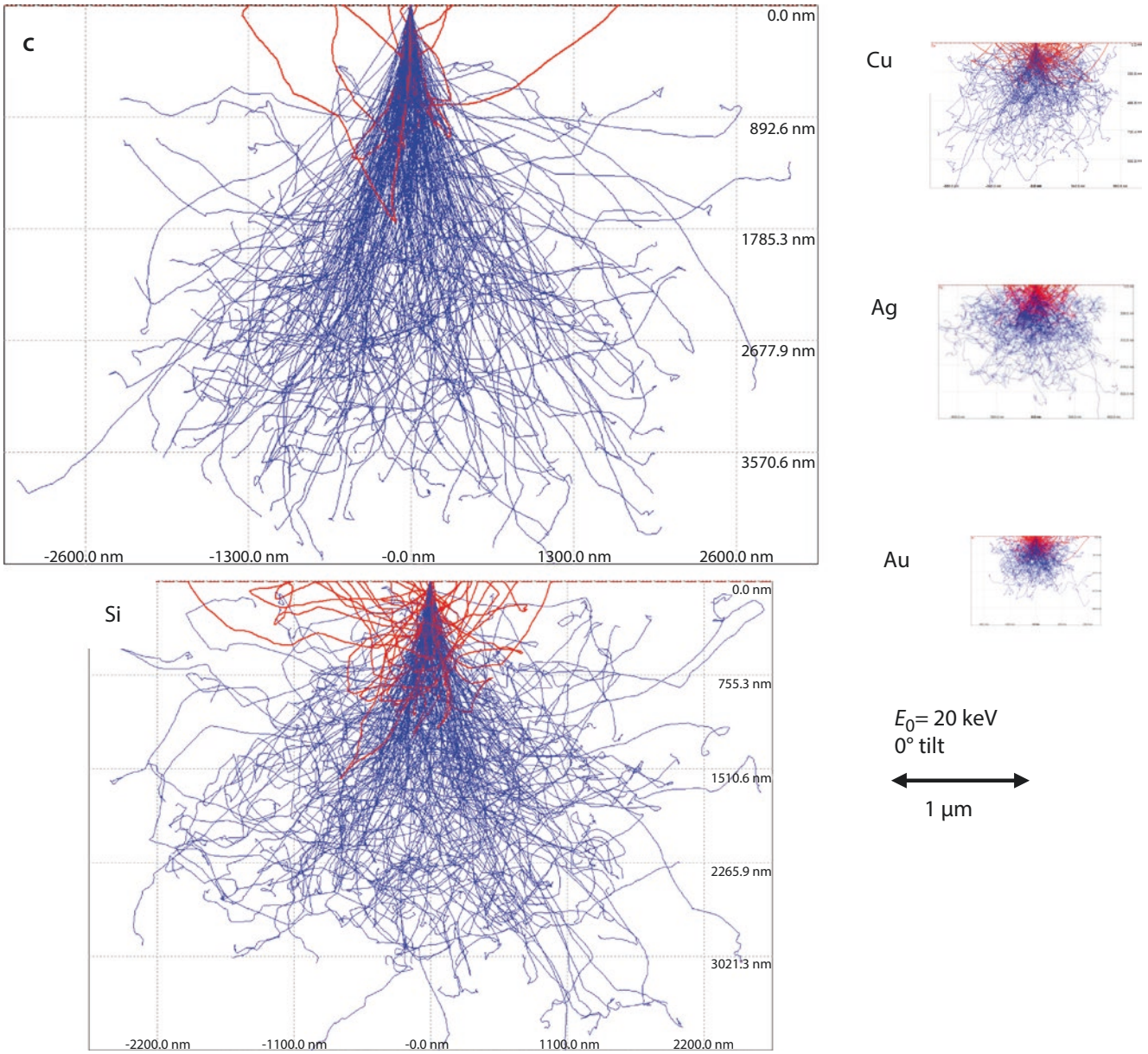

Fig. 1.8 Monte Carlo simulations for an incident beam energy of 20 keV and 0° tilt for C, Si, Cu, Ag, and Au, all shown at the same scale (CASINO Monte Carlo simulation)

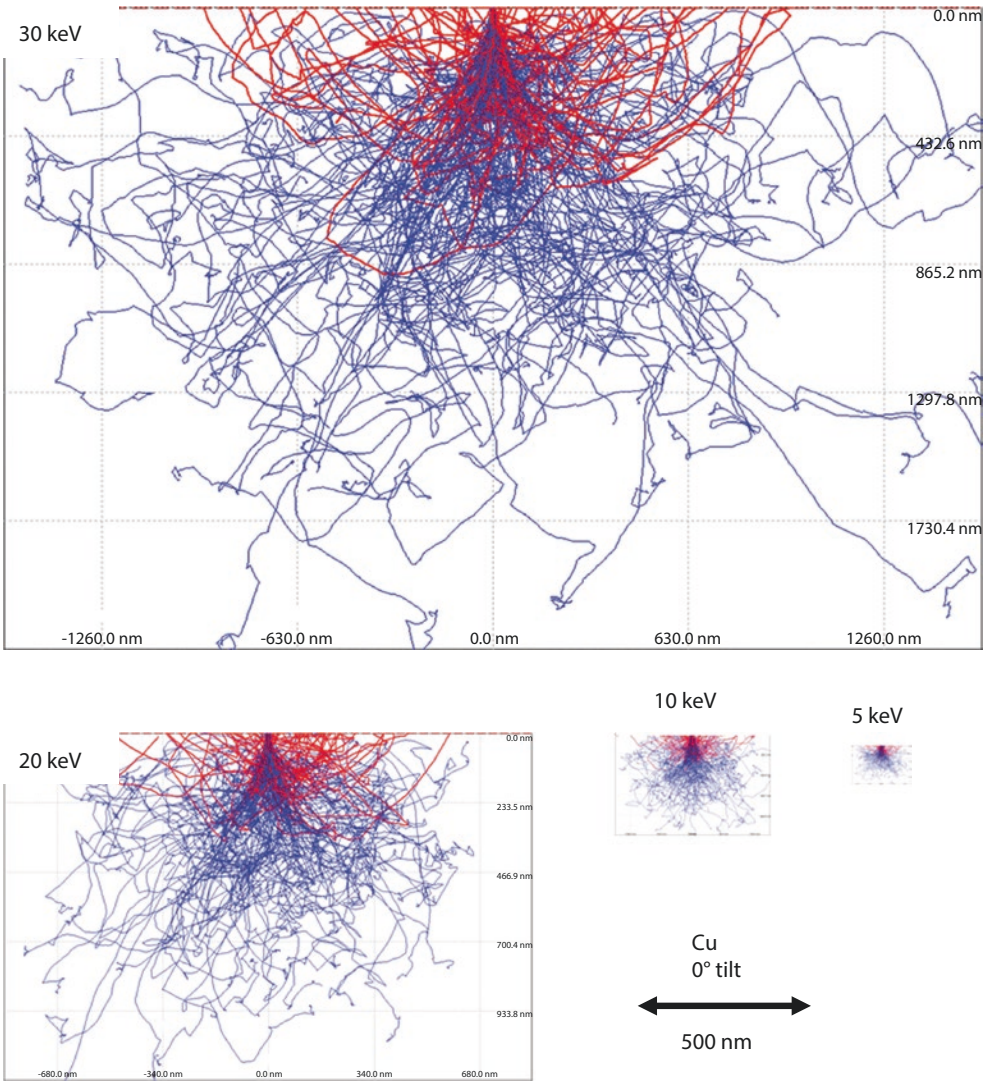

Fig. 1.9 Monte Carlo simulations for Cu, 0° tilt, incident beam energies 5, 10, 20, and 30 keV (CASINO Monte Carlo simulation)

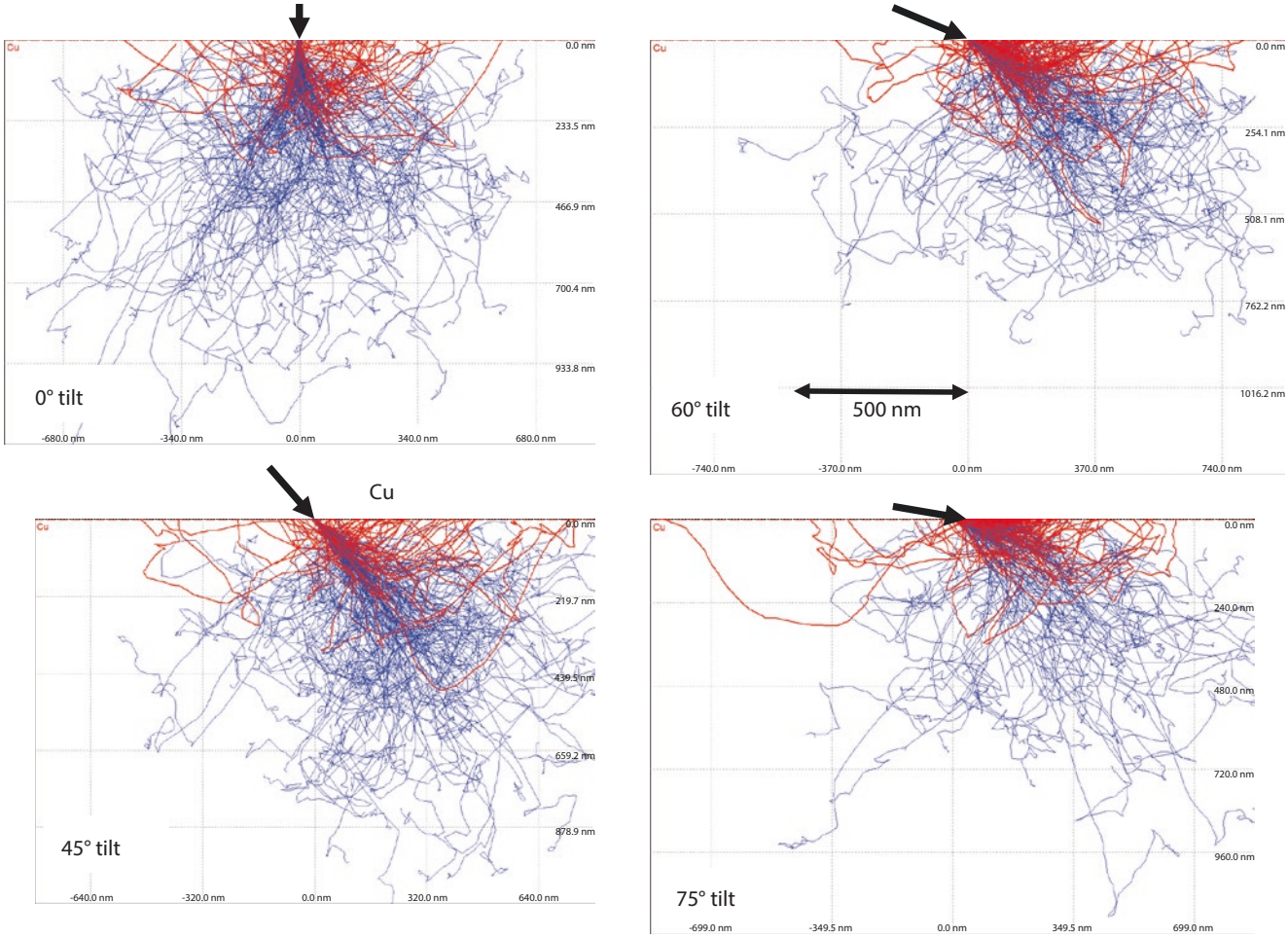

Fig. 1.10 Monte Carlo simulations for Cu, 20 keV, with various tilt angles (CASINO Monte Carlo simulation)

1.5 A Range Equation To Estimate the Size of the Interaction Volume

While the Monte Carlo simulation is a powerful tool to depict the complexity of the electron beam specimen interactions, it is often useful to have a simple estimate of the size. The Bethe range gives the maximum distance the beam electron can travel in the specimen, but this distance is measured along the complex trajectory that develops because of elastic scattering. Kanaya and Okayama (1972) developed a range equation that considered both inelastic and elastic scattering to give an estimate of the interaction volume as the radius of a hemisphere centered on the beam impact point that contained at least 95% of the trajectories:

$$R_{\mathrm{K-O}}\,(\mathrm{nm}) = 27.6\left(A / Z^{0.89}\rho\right)E_0^{1.67} \qquad (1.5)$$

Table 1.1 Kanaya–Okayama range

	5 keV (nm)	10 keV	20 keV	30 keV (μm)
C	450 nm	1.4 μm	4.5 μm	8.9 μm
Al	413 nm	1.3 μm	4.2 μm	8.2 μm
Fe	159 nm	505 nm	1.6 μm	3.2 μm
Ag	135 nm	431 nm	1.4 μm	2.7 μm
Au	85 nm	270 nm	860 nm	1.7 μm

where A is the atomic weight (g/mol), Z is the atomic number, ρ is the density (g/cm^3), and E_0 is the incident beam energy (keV). Calculations of the Kanaya–Okayama range are presented in Table 1.1. The Kanaya–Okayama range

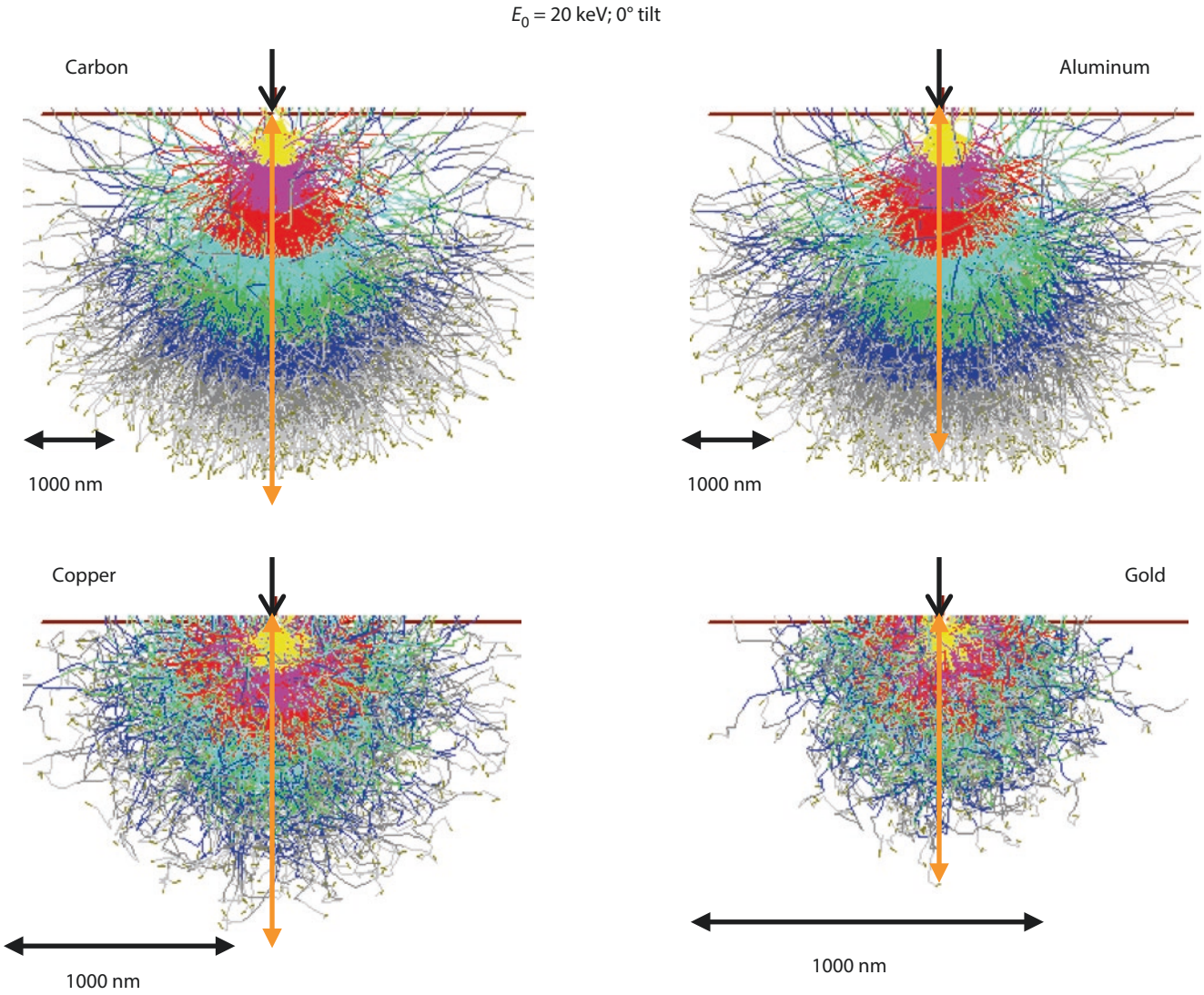

Fig. 1.11 Kanaya–Okayama range (*gold arrow*) superimposed on the interaction volume for C, Al, Cu, and Au at *E0* = 20 keV and 0° tilt (Joy Monte Carlo simulation)

is shown superimposed on the Monte Carlo simulation of the interaction volume in Fig. 1.11 and is plotted graphically in Fig. 1.12. It is, of course, simplistic to use a single numerical value of the range to describe such a complex phenomenon as the electron interaction volume with its varying contours of energy deposition, and thus the range equation should only be considered as a "gray" number useful for estimation purposes. Nevertheless, the Kanaya–Okayama range is useful as a means to provide scaling to describe the spatial distributions of the signals produced within the interaction volume: secondary electrons, backscattered electrons, and X-rays.

1

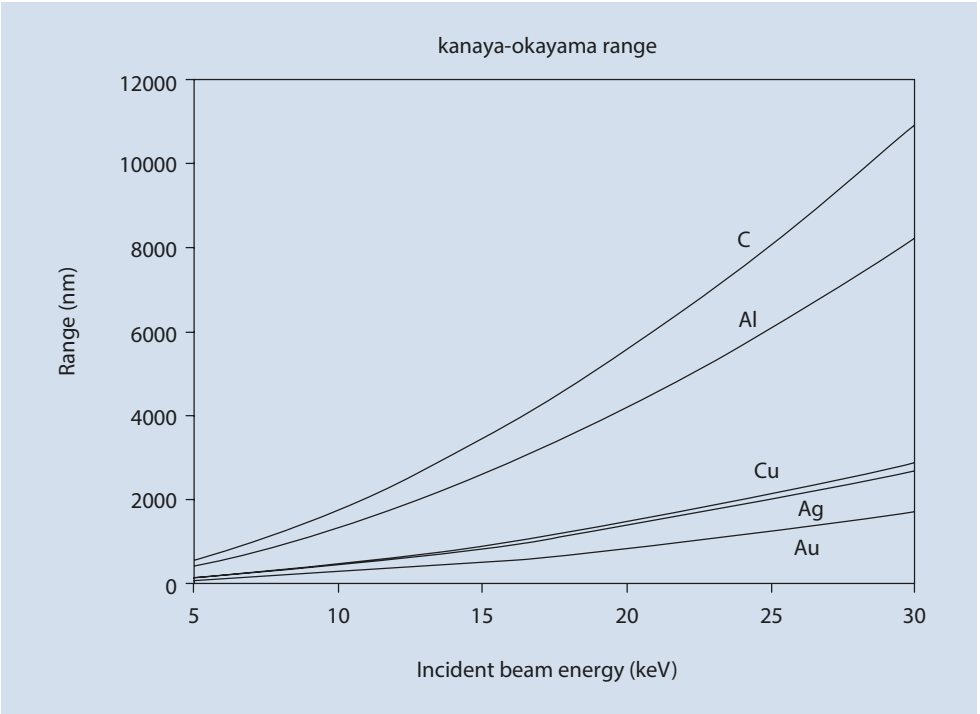

Fig. 1.12 Kanaya–Okayama range plotted for C, Al, Cu, Ag and Au as a function of E_0

References

Bethe H (1930) Theory of the transmission of corpuscular radiation through matter. Ann Phys Leipzig 5:325

CASINO ► http://www.gel.usherbrooke.ca/casino/What.html

Joy Monte Carlo ► http://web.utk.edu/~srcutk/htm/simulati.htm

Kanaya K, Okayama S (1972) Penetration and energy-loss theory of electrons in solid targets. J Phys D Appl Phys 5:43

NISTDTSA-II ► http://www.cstl.nist.gov/div837/837.02/epq/dtsa2/index.html